

DESIGN AND PERFORMANCE COMPARISON OF FOUR-POLE BRUSHLESS DC MOTORS WITH DIFFERENT POLE/SLOT COMBINATIONS

Cemil OCAK

Vocational College of Technical Sciences, Gazi University, Ankara, Turkey.
cemilocak@gazi.edu.tr

ABSTRACT

When the design process of the brushless motor is examined, attention must be paid to the correct choice of magnet material, internal or external rotor structure and the choice of core and winding structure. In addition to all these, the number of phases, the number of rotor poles, and the choice of slots configurations depending on them also have great importance. For this reason, to achieve optimum design, it is necessary to analyze all possible designs with different pole/slot configurations that can accommodate similar power and speed expectations. In this study, three different designs have been realized with different pole/slot configurations for four-pole, internal rotor brushless DC motors, which are frequently used in many different applications today. Designed motors have been analyzed with Finite Element Method to obtain the cogging torque, efficiency and active material costs. All motors that are analyzed have 100 W, 3000 rpm, 4/6, 4/12 and 4/15 pole/slot configurations respectively.

Keywords: brushless DC motor, pole/slot combinations, efficiency, internal rotor.

1. INTRODUCTION

Although the moment-speed characteristic is linear in DC motors, the most important disadvantage of this type of motors is the realization of excitation by using brush and collector assembly. Due to the mechanical commutation, the motor requires frequent maintenance. Brushless DC motors (BLDC) have the moment-speed characteristic of brushed DC motors and eliminates the disadvantage of brush and collector mechanism by using electronic commutation [1-2].

Recent developments in material science have allowed the production of magnets with high energy density. With the use of magnets which have high BH_{max} products, it was possible to obtain more power in a smaller volume. In addition, there has been a reduction in the cost of the switching elements due to the development of semiconductor technology. BLDCs have become more attractive with the increasing simplicity and reliability of electronic components, falling costs, and developments in material technology [3]. BLDCs are almost maintenance-free and long-life electrical machines with a low moment of inertia. The absence of rotor windings in this type of motors lead to the absence of rotor copper losses and therefore to high efficiency. The BLDCs have a higher torque density than an asynchronous motor or brush motor for the same size [4].

In the literature, effect of different pole slot combinations in the linear motor [5], in the brushless doubly-fed generator [6], in the interior permanent magnet synchronous motor [7-8], in the surface-mounted permanent magnet machine [9], and in the axial flux BLDC motor [10] have been discussed. Also, cogging torque parameter has been examined for different pole/slot combinations (4/6, 8/12 and 10/12) of permanent magnet synchronous motor. A proper cogging torque value can be obtained without any additional manufacturing process [11].

The relationship between the number of poles and slots in BLDC motors is quite popular. Even though it is thought that the today's mass-production motors have the pole/slot configurations which present the best performance, in fact, various computer-aided analyzes show that this is not always the case. For example, most 4-pole BLDC motors are produced as 12 stator slots. However, this type of design results in a very high cogging torque and large end turn lengths and thus high copper losses. In addition, the cost of winding and labour increases. For a lower cogging torque and a cost target, 4 pole/6 slot configuration can be preferred. If a motor with low cogging torque and a sinusoidal back emf is desired, 4 pole/15 slot configuration will be the best choice compared to the other alternatives mentioned above. In this study, as mentioned above, three BLDC motors rated 100W, and 3000 rpm have been designed with 4/6, 4/12 and 4/15 pole/slot configurations. Finite element method (FEM) has been used to analyze the proposed designs. As a result of performed analyzes, cogging torques, phase and line voltage waveform of motors have been obtained and compared according to the different pole/slot numbers given in the study. Thus, the effects of different pole/slot configurations have been obtained by computer-aided simulations for these motors which are widely used.

2. MATHEMATICAL MODEL OF BRUSHLESS DC MOTORS

The instantaneous power produced by the BLDC motor is equal to the back electromotive force multiplied by phase current. This is the power that is transferred from stator to rotor. When the friction losses are extracted from the transmitted power, the net power from the motor shaft can be determined. Since the friction losses of the BLDC motor are very small, the power value can be written as in Equation 1.

$$P_e = i_a e_a + i_b e_b + i_c e_c \quad (1)$$

Considering the 120° phase difference between the phases, the expression of the back electromotive force given in Equation 1 can be written as Equation 2.

$$\begin{aligned} e_a &= \omega \lambda(\theta) \\ e_b &= \omega \lambda\left(\theta - \frac{2\pi}{3}\right) \\ e_c &= \omega \lambda\left(\theta + \frac{2\pi}{3}\right) \end{aligned} \quad (2)$$

The resulting back electromotive force is in the form of a trapezoidal wave, which varies depending on the position. The value of the back electromotive force depends on the number of turns, magnetic field strength, rotor speed, and position. The equivalent circuit of the 3-phase star-connected BLDC motor is given in Figure 1.

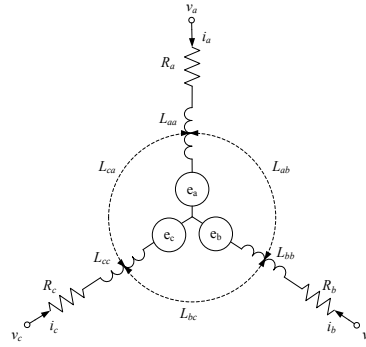


Figure 1. Three-Phase Equivalent Circuit of BLDC Motors

Voltage equation for the phase a is given in Equation 3 according to the equivalent circuit.

$$v_a = i_a R_a + L_a \frac{d i_a(t)}{dt} + e_a \quad (3)$$

The voltage equation for each phase of BLDC motor is expressed as Equation 4 [12-14].

$$\begin{bmatrix} v_a \\ v_b \\ v_c \end{bmatrix} = \begin{bmatrix} R_a & 0 & 0 \\ 0 & R_b & 0 \\ 0 & 0 & R_c \end{bmatrix} \begin{bmatrix} i_a \\ i_b \\ i_c \end{bmatrix} + \begin{bmatrix} L_{aa} & L_{ab} & L_{ca} \\ L_{ab} & L_{bb} & L_{bc} \\ L_{ca} & L_{bc} & L_{cc} \end{bmatrix} \frac{d}{dt} \begin{bmatrix} i_a \\ i_b \\ i_c \end{bmatrix} + \begin{bmatrix} e_a \\ e_b \\ e_c \end{bmatrix} \quad (4)$$

3. ELECTROMAGNETIC FINITE ELEMENT ANALYSIS

Analysis of electrical machines involves the solution of interrelated problems. Applying the finite element method (FEM) in the analysis of electrical machines enables the designer to obtain the behavior of the machine. It is possible to determine the electromagnetic parameters with a very high accuracy by applying a FEM method. In addition, applying this method gives the designer a considerable advantage over time and cost [15-16]. The region to be solved in FEM is divided into a small number of finite regions. The desired value is assumed to be continuous over these small regions. In addition, it is assumed that the fundamental differential equation expressing the change of field is also valid on each element. In order to obtain the solution at a point in the region, the contributions of the elements surrounding the point must be taken into account.

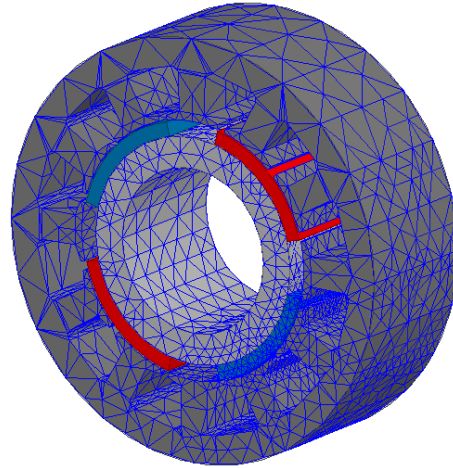


Figure 2. Mesh View of 4 Pole /12 Slot Motor

Therefore, the values of the corner points of all the elements in the region are chained together. As a result, a group of linear equation as much as the number of nodes is obtained. By solution of this equation set, the desired ones are calculated [16-17]. The mesh structure of the proposed 12-slot motor is shown in Figure 2.

3.1. Analysis Model and Study of Proposed Design Combinations

In this section of the study, designs of the BLDC motor which is rated 100 W and 3000 rpm in different pole/slot combinations have been performed and their performances have been examined. Design parameters and materials of the motors are given in Table 1.

Table 1. Design Parameters

Pole / Slot Combination		4 pole/6 slot	4 pole/12 slot	4 pole/15 slot
Stator	Outer diameter (mm)	90	90	90
	Inner diameter (mm)	55	55	55
	Length (mm)	30	30	30
	Core Material	M270-35A	M270-35A	M270-35A
Rotor	Outer diameter (mm)	54.2	54.2	54.2
	Inner diameter (mm)	35	35	35
	Length (mm)	30	30	30
	Core Material	ST37	ST37	ST37
Magnet	Type	N40UH	N40UH	N40UH
	Thickness (mm)	3	3	3
	Embrace	0.7	0.7	0.7
Slot	Slot clearance (mm)	5	2	2
	Width (mm)	28	13	9
	Net Slot Area (mm ²)	233.03	106.53	72.53

When Table 1 is examined, it is seen that the materials and physical properties of the stator, rotor, and magnet are arranged to be the same for each design. The slot geometry has been arranged according to the different number of slots providing a maximum slot fill factor for each design. Thus, other parameters of the motor have not been changed to obtain a fair

comparison while performing a comparative analysis. The view of the different pole/slot configurations of the designs has been presented in Figure 3. As can be seen from the Figure 3, rotor structures, stator inner and outer diameters and air gap distances are kept the same for the different configurations.

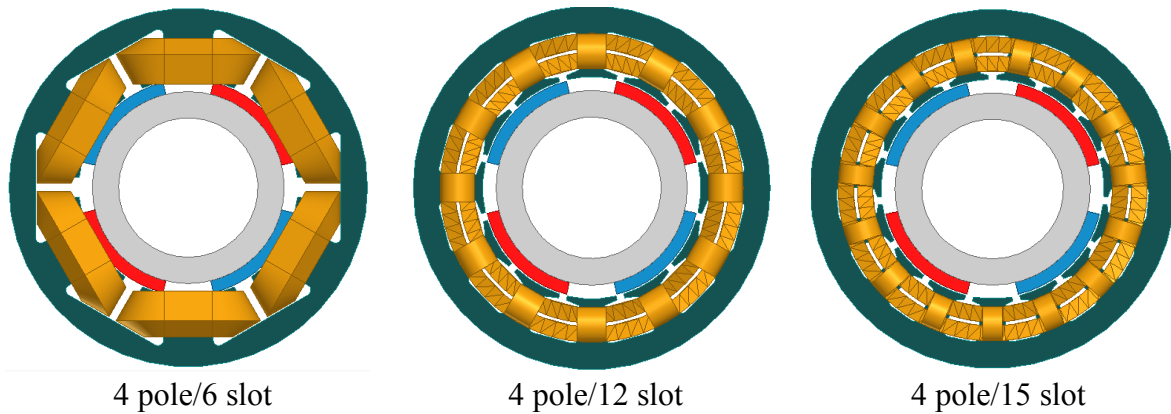


Figure 3. Views of Different Pole/Slot Configurations

3.2. Comparison of Load Performances and Flux Density Distributions

In this section, performance values and flux distributions have been examined comparatively by analyzing the motors at rated load and unloaded condition. The simulation results of full and no-load conditions are given in Table 2.

Table 2. Performance Values of Motors

Parameters		4 pole/6 slot	4 pole/12 slot	4 pole/15 slot
Full-load	Output power (W)	100	100	100
	Efficiency (%)	85.32	85.16	85.29
	Rated torque (Nm)	0.304	0.312	0.308
No-load	Cogging torque (Nm)	0.107	0.204	0.05
	Stator teeth flux density (T)	1.73	1.79	1.71
	Rotor yoke flux density (T)	1.65	1.71	1.74
	Stator slot fill factor (%)	51.0	51.3	51.6

When the output power values in Table 2 are examined, it is seen that all motors have been loaded to produce the same output power. The designs were aimed to provide the maximum slot fill factor and similar efficiency values to obtain balanced copper loss which is an important factor of efficiency between different designs. When the cogging torques values are compared, it is seen that the 4 pole/12 slot configuration has the highest cogging torque value. The lowest cogging torque value has been obtained in 4 pole/15 slot configuration. However, the winding and labour cost of this motor is higher than the other configurations. In the case of a cost-effective motor expectation, the 4 pole/6 slot motor can be preferred even if it has a high cogging torque compared to the 4/15 structure. When no load condition considered, it is also seen that stator and rotor flux densities are within the limit in each design and it can be modified by geometric changes. As mentioned before, the FEM is a very effective and frequently used method in the calculation of magnetic flux distributions. In electric machines, the magnetic field

calculations are expressed by Maxwell's equations and the flux distribution obtained by the 3D analysis given in Figure 4 are found by the following equations [17-19].

$$\begin{aligned} \nabla \times \vec{H} &= \vec{J} \\ \nabla \times \vec{E} &= -\frac{\partial B}{\partial t} \end{aligned} \tag{5}$$

The magnetic vector potential can be expressed in terms of magnetic flux density in Equation 6.

$$\vec{B} = \nabla \times \vec{A} \tag{6}$$

The basic formulation of the vector potential for the magnetic field is expressed by Equation 7.

$$\nabla \times (\nu \nabla \times \vec{A}) = \vec{J} \tag{7}$$

$$\frac{\partial}{\partial x} \left(\nu \frac{\partial A}{\partial x} \right) + \frac{\partial}{\partial y} \left(\nu \frac{\partial A}{\partial y} \right) + \frac{\partial}{\partial z} \left(\nu \frac{\partial A}{\partial z} \right) = -\vec{J} \tag{8}$$

The magnetic flux density value is obtained from Equation 9.

$$B = \sqrt{B_x^2 + B_y^2 + B_z^2} \tag{9}$$

The magnetic flux distributions obtained by magneto-static analyzes are given in Figure 4. Only magnets were defined as a flux source to obtain no load condition. The upper limit of the color map for the flux density distributions is defined as 2T. Considering this definition, it can be seen that the flux densities of the cores are in line with the selected material and the limit.

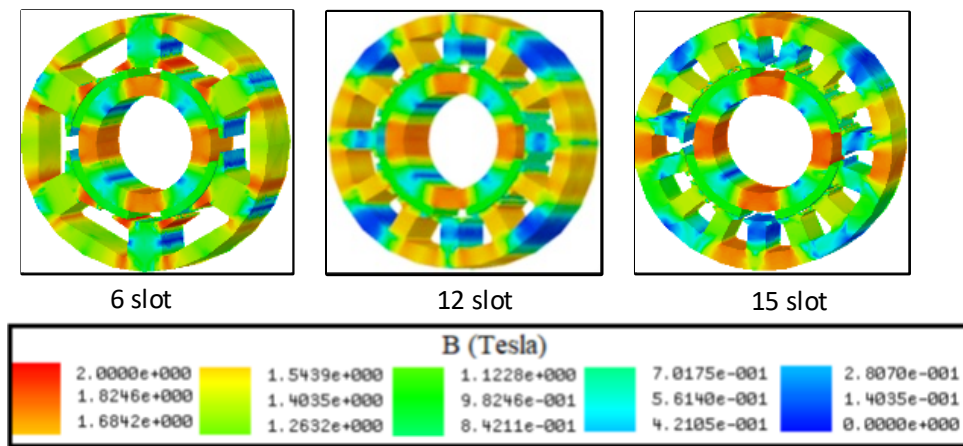


Figure 4. Magnetic Flux Density Distributions of Proposed Configurations

3.3. Cogging Torque

Cogging torque is the torque generated by the interaction between the stator slots and rotor magnets when no current applied on permanent magnet machines. The cogging torque is undesirable for electric machines because it causes noise and vibration by forcing rotation of

the rotor. The change of the cogging torque according to the electrical position of the rotor for each configuration is given in Figure 5. The lowest cogging torque value has been obtained in 4 pole/15 slot structure. Since the 4-pole/12-slot configuration has a very high cogging torque compared to other designs, this configuration should not be preferred. The 4-pole/6-slot configuration is acceptable for a cost-priority design.

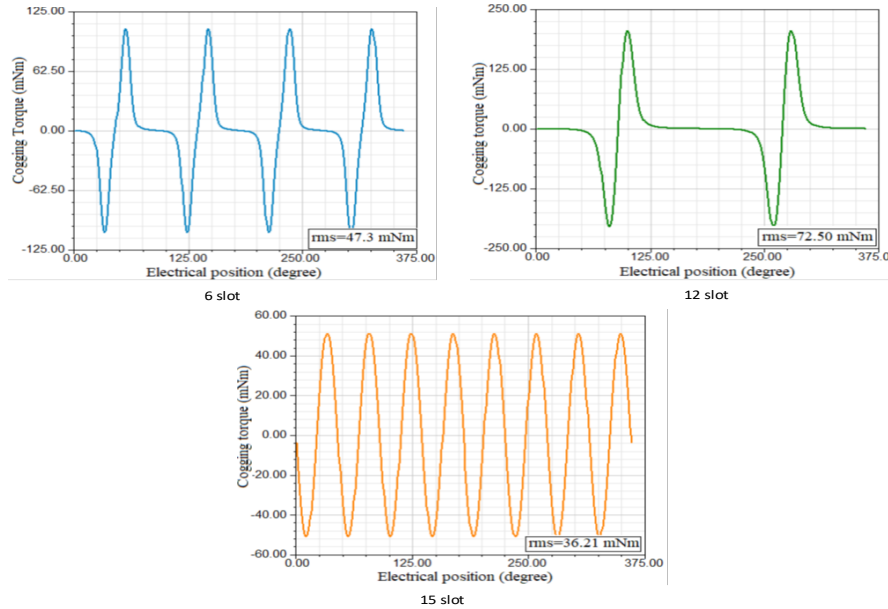


Figure 5. Cogging Torque Values for the Different Pole/Slot Configurations

3.4. Induced Coil Voltage

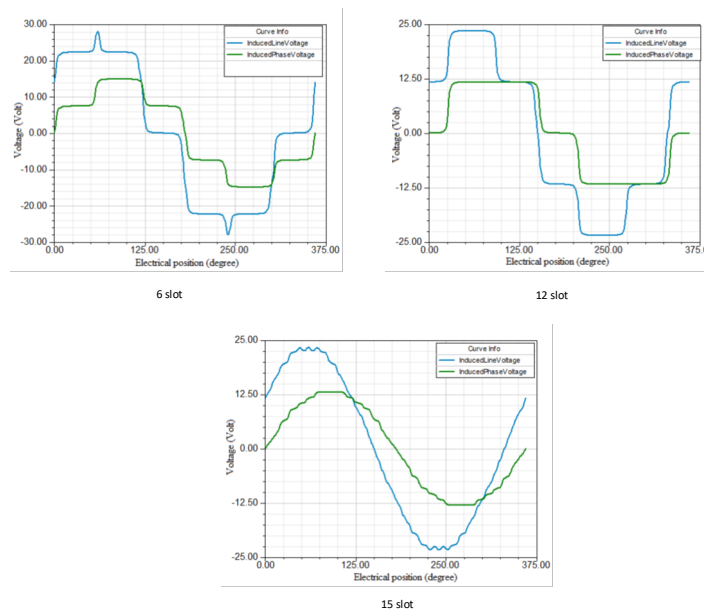


Figure 6. Line and Phase Voltage Waveforms for Different Pole/Slot Combinations

The voltage equations of the BLDC motors have been previously given in Equations 3 and 4. According to the electrical position of the rotor, phase and line voltage values of phase A of the designed motor are given in Figure 6. The waveform of the induced voltage and air gap flux density are important in terms of core losses, especially for the high-speed motor designs. The

induced voltage waveforms of 4 pole/6 slot and 4 pole/12 slot configurations are far from the sinusoidal form. Furthermore, due to their high harmonic content, these designs should not be the first priority in applications with high-efficiency targets. In such a case, the 4-pole/15-slot configuration provides the best waveform with an almost sinusoidal waveform. This configuration offers superior performance values than the other two configurations when winding and labour cost are neglected.

4. CONCLUSION

In the study, the designed motors are rated 100 W, 3000 rpm and have four-pole internal rotor structure. These machines have high torque density, robust structure, low loss, and low manufacture cost. In the design phase, pole/slot number has a dominant effect on machine performance. Three brushless DC motors have been compared in this study for revealing the effect of the pole/slot configurations on the characteristics. Designed motors have been analyzed with FEM Method. Each motor has 4 pole and 6, 12 and 15 stator slots respectively. The lowest cogging torque value has been obtained in 4 pole/15 slot configuration compared to other designs. Therefore, the minimum torque fluctuation has been obtained in 4 pole/15 slot configuration. 4 pole/12 slot configuration has the worst performance values in terms of both cogging torque and induced voltage waveforms. The 4-pole / 6-slot configuration has a relatively low cogging torque and total cost. Therefore, these motors are often preferred in many applications such as an electric screwdriver and similar power tools. On the other hand, where more specific working conditions such as the defense industry and where efficiency is more important, despite a small increase in cost, a 4-pole/15-slot configuration is preferable because of its low cogging torque and sinusoidal waveform.

Author Note: This research work was presented as an oral paper at the 3rd international Energy & Engineering Congress (UEMK2018).

NOMENCLATURE

$v_{a,b,c}$: Voltages of phases a, b, and c
$i_{a,b,c}$: Currents of phases a, b, and c
$R_{a,b,c}$: Winding resistances of phases a, b, and c
$e_{a,b,c}$: Induced back-electromotive force
L_{aa}, L_{bb}, L_{cc}	: Total inductance of phase windings
L_{ab}, L_{bc}, L_{ca}	: Mutual inductances between phase windings
\vec{H}	: Magnetic field intensity
\vec{J}	: Current density
\vec{E}	: Electric field intensity
\vec{B}	: Magnetic flux density
\vec{A}	: Magnetic vector potential

REFERENCES

- [1] Hanselman, D. Brushless permanent magnet motor design. 2nd ed. OH: Magna Physics Publishing, 2006.
- [2] Saygın, A., Ocak, C., Dalcalı, A., Çelik, E. Optimum rotor design of small PM BLDC motor based on high efficiency criteria. *ARNP Journal of Engineering and Applied Sciences* 2015; 10(19): 9127-9132.
- [3] Bayındır, R., Ocak, C., Topaloğlu, İ. Investigation of the effect of magnet thickness on output power and torque of PM BLDC machines using parametric approach method. In *Proceedings of POWERENG 2011*; 11-13 May 2011; Malaga, Spain. pp. 1-4.
- [4] Ehsani, M., Gao, Y., Gay, S. Characterization of electric motor drives for traction applications. *IECON'03. 29th Annual Conference of the IEEE Industrial Electronics Society*; Roanoke, VA, USA, 2003, pp. 891-896 vol.1
- [5] Yuan, M., Niu, S. Design and analysis of a novel modular linear double-stator biased flux machine. *IEEE Transactions on Magnetics, Early Access*, 2018: 1-5.
- [6] Zhang, F., Yu, S., Wang, Y., Jin, S., Jovanovic, M.G. Design and performance comparisons of brushless doubly fed generators with different rotor structures. *IEEE Transactions on Industrial Electronics*, 2019: 66(1), 631-640. doi: 0.1109/TIE.2018.2811379
- [7] Carraro, E., Zhang, S., Koch, M. Design and performance comparison of fractional slot concentrated winding spoke type synchronous motors with different slot-pole combinations. *IEEE Transactions on Industry Applications*, 2018: 54(3), 2276-2284.
- [8] Jun, H.W., Seol, H.S., Lee, J. Effect of pole–slot combination on eddy-current formation in pmsm rotor assembly including retaining plate structure. *IEEE Transactions on Magnetics*, 2017: 53(11).
- [9] Zhu, Z.Q., Wu, J., Modh Jamil, M.L. Influence of pole and slot number combinations on cogging torque in permanent-magnet machines with static and rotating eccentricities. *IEEE Transactions on Industry Applications*, 2014: 50(5), 3265-3277.
- [10] Jafarishiadeh, S., Ardebili, M., Marashi, A.N. Investigation of pole and slot numbers in axial-flux pm BLDC motors with single-layer windings for electric vehicles. *24th Iranian Conference on Electrical Engineering (ICEE)*, 2016, Shiraz, Iran.
- [11] Lee, S.J., Kim, S.I., Hong, J.P. Characteristics of PM synchronous motors according to pole-slot combinations for eps applications. *International Journal of Automotive Technology*, 2014: 15(7), 1183–1187. doi: 10.1007/s12239-014-0123-6
- [12] Çelik, E., Öztürk, N. A new fuzzy logic estimator for reduction of commutation current pulsation in brushless DC motor drives with three-phase excitation. *Neural Comput & Application*, 2017: 1-10. doi: 10.1007/s00521-017-3083-8
- [13] Krishan, R. *Electric motor drives: modeling, analysis and control*. New Jersey: Prentice Hall, Inc. 2001.

- [14] Aydoğdu, Ö. Sensorless control of brushless dc motors by means of genetic based fuzzy controller. PhD Thesis, Selçuk University, Konya, Turkey 2006.
- [15] Hameyer, K., Belmans, R. Numerical modelling and design of electrical machines and devices. Southampton, Boston: WIT Press, 1999.
- [16] Dalcalı, A., Kurt, E., Çelik, E., Öztürk., N. Cogging torque reduction by using the skewing and separated magnet techniques. 6th Eur. Conf. Ren. Energy Sys., 2018: 24(6), Istanbul, Turkey.
- [17] Dalcalı, A., Akbaba, M. Comparison of 2D and 3D magnetic field analysis of single-phase shaded pole induction motors. Engineering Science and Technology, An International Journal, 2016: 19(1), 1–7. doi: 10.1016/j.jestch.2015.04.013
- [18] Ho, S. L., Fu, W. N. Review and future application of finite element methodes in induction motors. Electric Machines & Power Systems, 1998: 26 (2), 111–125.
- [19] Dadpour, A., Ansari, K. Conversion of shaded-pole induction motor to switched reluctance motor and effects of pole shoe and notch on SRM noise", IEEE XXXIII International Scientific Conference Electronics and Nanotechnology, 2013, Kiev.